

Supplemental Material

S.1 SUPPLEMENTARY NOTE 1: Details of HRF

S.1.1 Algorithm description via pseudocode

Algorithm 1 Hadamard Random Forest (HRF)

Require: Number of qubits N_q , sample size for each circuit $N_{\text{samp.}}$, number of trees N_{tree}

Ensure: Reconstruct real state vector $|\psi\rangle \in \mathbb{R}^{2^{N_q}}$

▷ 1. Collect samples

```

1: Prepare  $N_{\text{samp.}}$  copies of  $|\psi\rangle$  using  $U_{\text{prep.}}$ 
2: Measure all  $N_q$  qubits in  $\sigma_z$  basis
3: for all  $j \in \{0, \dots, 2^{N_q} - 1\}$  do
4:    $|\tilde{\psi}_j|^2 \leftarrow$  empirical frequency in basis  $|j\rangle$ 
5: end for
6: for  $k = 0$  to  $N_q - 1$  do
7:   Prepare  $N_{\text{samp.}}$  copies of  $|\psi\rangle$  using  $U_{\text{prep.}}$ 
8:   Measure the  $(N_q - k - 1)$ -th qubit in  $\sigma_x$  basis
9:   Measure the rest qubits in  $\sigma_z$  basis
10:  for all  $j \in \{0, \dots, 2^{N_q} - 1\}$  do
11:     $|\tilde{\psi}_j^k|^2 \leftarrow$  empirical frequency in basis  $|j\rangle$ 
12:  end for
13: end for

```

▷ 2. Build random forest

```

14: for  $i = 1$  to  $N_{\text{tree}}$  do
15:    $T_i \leftarrow$  a random spanning tree on  $\mathcal{Q}_{N_q}$  using BFS
16:   Initialize root sign  $s_0^{(i)} \leftarrow +1$ 
17:   for all unique path from node  $0 \rightarrow j$  in  $T_i$  do
18:     for all valid  $(n, k)$  along path do
19:       Compute relative signs
20:        $s_{n, n+2^k}^{(i)} \leftarrow \text{sgn}(2|\tilde{\psi}_n^k|^2 - |\tilde{\psi}_n|^2 - |\tilde{\psi}_{n+2^k}|^2)$ 
21:        $s_j^{(i)} \leftarrow s_{j, j-2^k}^{(i)} \times \dots \times s_{2^k, 0}^{(i)} \times s_0^{(i)}$ 
22:     end for
23:   end for
24: end for

```

▷ 3. Majority voting

```

25: for all  $j \in \{0, \dots, 2^{N_q} - 1\}$  do
26:    $s_j \leftarrow \text{sgn}\left(\sum_{i=1}^{N_{\text{tree}}} s_j^{(i)}\right)$ 
27: end for

```

▷ 4. Reconstruct state

```

28: for all  $j \in \{0, \dots, 2^{N_q} - 1\}$  do
29:    $|\tilde{\psi}_j| \leftarrow \sqrt{|\tilde{\psi}_j|^2}$ 
30:    $\tilde{\psi}_j \leftarrow s_j \times |\tilde{\psi}_j|$ 
31: end for
32: return  $|\tilde{\psi}\rangle$ 

```

S.1.2 Quantum circuit construction

We use the hardware-efficient ansatz to prepare real-valued states as shown in [fig. S1](#). The parameters are chosen uniformly from the interval $[-\pi/2, \pi/2]$.

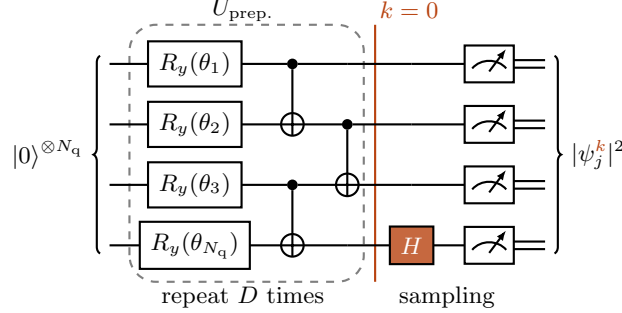


FIG. S1: State preparation and measurement circuits for HRF. The largest case on the IBM hardware benchmark [section 3.3.1](#) contains 36 CZ gates.

S.1.3 Hardware calibration data

[Table S1](#) shows the hardware calibration data used throughout the manuscript.

Qubit	T_1 (μ s)	T_2 (μ s)	Meas. error ε	2Q gate error ε_{2q}
Q_0	184	101	4.64×10^{-3}	2.74×10^{-3}
Q_1	188	237	4.88×10^{-3}	2.69×10^{-3}
Q_2	216	173	4.39×10^{-3}	3.02×10^{-3}
Q_3	171	248	6.34×10^{-3}	3.35×10^{-3}
Q_4	142	111	1.56×10^{-2}	3.35×10^{-3}
Q_5	197	31	5.62×10^{-3}	3.48×10^{-3}
Q_6	170	152	9.28×10^{-3}	5.54×10^{-3}
Q_7	140	138	4.15×10^{-3}	3.42×10^{-3}
Q_8	154	111	1.29×10^{-2}	3.65×10^{-3}
Q_9	98	57	4.64×10^{-3}	/
Avg.	166	136	7.24×10^{-3}	3.47×10^{-3}

TABLE S1: Device properties of `ibm_fez` at the time each experiment reported in this paper was performed. The readout length is $t_{\text{mea.}} = 1560$ ns and native 2Q gate (CZ) with pulse length $t_{2q} = 84$ ns for all qubits.

S.2 SUPPLEMENTARY NOTE 2: MEASUREMENT SCHEMES

S.2.1 Quantum Amplitude Estimation

Compared to quantum amplitude estimation (QAE) [\[12, 13\]](#), HRF employs shallow circuits with easily implementable gates. QAE is optimal for estimating a specific amplitude or a few dominant

amplitudes. Still, it requires deep, coherent circuits with controlled unitaries, which are challenging to implement and prone to errors. HRF offers a more scalable alternative that recovers all the amplitudes simultaneously instead of running QAE sequentially, making HRF well-suited for near-term quantum applications. [table S2](#) provides a detailed comparison of HRF and QAE.

Feature	QAE	HRF (this work)
Objective	Estimate single amplitude of general complex quantum states	Reconstruct full state vector of real-valued quantum states
Circuit Depth	Deep (uses Grover-like subroutines)	Shallow (single-layer Hadamards)
Measurements	Controlled unitaries with ancilla	σ_z, σ_x only
Qubit Overhead	$N_q + 1$ or more (ancilla + control)	N_q
Sample Complexity	Optimal $\mathcal{O}(1/\epsilon)$	Trade more samples for shallow circuits
NISQ Suitability	Low; Error-prone	High; Error-robust

TABLE S2: Comparison between Quantum Amplitude Estimation and Hadamard Random Forest.

S.2.2 Quantum state overlap estimation

Here, we show a concrete example of how HRF can simplify the task of estimating the overlap $S = |\langle\psi|\phi\rangle|^2$ between two unknown quantum states $|\psi\rangle$ and $|\phi\rangle$. Such a task has applications in quantum machine learning [48, 49] and cross-platform verification [50]. A widely adopted approach to this problem is the SWAP test [46], which involves applying a controlled-SWAP operation and measuring an ancillary qubit (see [fig. S2](#)). However, the SWAP test requires direct preparation and entanglement between the two states, making its implementation resource-intensive on near-term devices.

The HRF offers an alternative method for estimating state overlap. Instead of requiring entanglement between $|\psi\rangle$ and $|\phi\rangle$, HRF reconstructs each state independently and computes their overlap classically via post-processing of reconstructed amplitudes. This approach significantly reduces the circuit size by half. It also eliminates the need for controlled-SWAP operations, making it more scalable and implementable for near-term quantum hardware. In larger circuits, like the SWAP test, noise accumulates. Since HRF uses smaller circuits, it is more resilient to noise and can integrate well-established error mitigation methods such as SPAM error cancellation, as demonstrated in this work. The lower circuit complexity also opens up the possibility of further noise reduction techniques.

Regarding sample complexity and scalability, suppose there are R states. The swap test requires circuits involving all R^2 pairs of states, whereas HRF only needs to characterize each of the R states individually, leading to a quadratic speedup in terms of the number of states. We note, however, that HRF shifts the expensive cross-state quantum operations into classical post-processing, with a trade-off of potentially more measurement shots. Thus, HRF is more advantageous for near-term devices where minimizing quantum circuit depth is crucial. Beyond state overlap estimation, the advantage brought by HRF can also generalize to other tasks involving multi-state property estimation, such as entanglement estimation [51, 52].

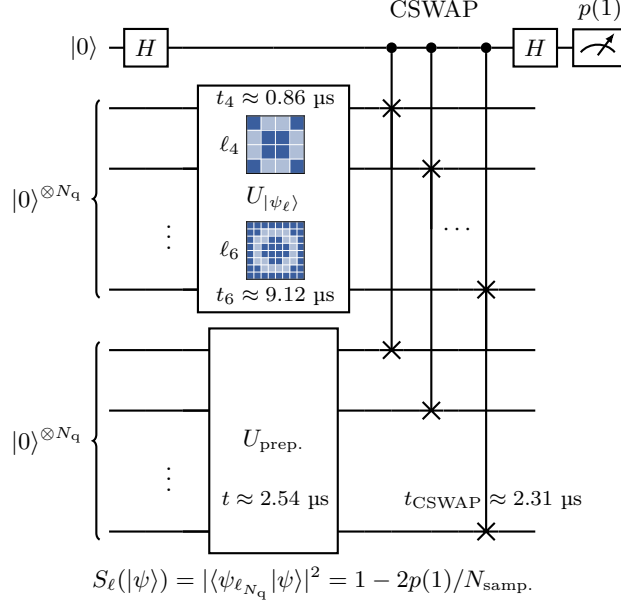


FIG. S2: SWAP test for estimating overlap $S_\ell(|\psi\rangle)$ with transpiled execution time on `ibm_fez` for each block.

In this study, we apply the SWAP test to estimate overlap that resembles a numerical integration over the path ℓ_{N_q} . More specifically, the index state that encodes the 4-qubit path ℓ_4 is shown below

$$\begin{aligned}
 |\psi_{\ell_4}\rangle = & \frac{1}{2\sqrt{2}} (|0001\rangle + |0010\rangle + |0100\rangle + |0111\rangle \\
 & + |1000\rangle + |1011\rangle + |1101\rangle + |1110\rangle).
 \end{aligned} \tag{S1}$$

This happens to be a stabilizer state with $M_2(|\psi_{\ell_4}\rangle) = 0$ but more generally $|\psi_{\ell_6}\rangle$ is not.